Aalborg Universitet

AALBORG UNIVERSITY
DENMARK

High-Performance Constant Power Generation in Grid-Connected PV Systems

Sangwongwanich, Ariya; Yang, Yongheng; Blaabjerg, Frede

Published in:
IEEE Transactions on Power Electronics

DOI (link to publication from Publisher):
10.1109/TPEL.2015.2465151

Publication date:
2016

Document Version
Early version, also known as pre-print

Link to publication from Aalborg University

Citation for published version (APA):
Sangwongwanich, A., Yang, Y., & Blaabjerg, F. (2016). High-Performance Constant Power Generation in Grid-Connected PV Systems. *IEEE Transactions on Power Electronics*, *31*(3), 1822-1825. https://doi.org/10.1109/TPEL.2015.2465151

General rights
Copyright and moral rights for the publications made accessible in the public portal are retained by the authors and/or other copyright owners and it is a condition of accessing publications that users recognise and abide by the legal requirements associated with these rights.

- Users may download and print one copy of any publication from the public portal for the purpose of private study or research.
- You may not further distribute the material or use it for any profit-making activity or commercial gain
- You may freely distribute the URL identifying the publication in the public portal -

Take down policy
If you believe that this document breaches copyright please contact us at vbn@aub.aau.dk providing details, and we will remove access to the work immediately and investigate your claim.

Downloaded from vbn.aau.dk on: April 24, 2024

Letters

High-Performance Constant Power Generation in Grid-Connected PV Systems

Ariya Sangwongwanich, Yongheng Yang, *Member, IEEE,* and Frede Blaabjerg, *Fellow, IEEE*

***Abstract*—An advanced power control strategy by limiting the maximum feed-in power of PV systems has been proposed, which can ensure a fast and smooth transition between maximum power point tracking and Constant Power Generation (CPG). Regardless of the solar irradiance levels, high-performance and stable operation are always achieved by the proposed control strategy. It can regulate the PV output power according to any set-point, and force the PV systems to operate at the left side of the maximum power point without stability problems. Experimental results have verified the effectiveness of the proposed CPG control in terms of high accuracy, fast dynamics, and stable transitions.**

***Index Terms*—Active power control, constant power control, maximum power point tracking, PV systems, power converters.**

I. Introduction

CURRENTLY, Maximum Power Point Tracking (MPPT) operation is mandatory for grid-connected PV systems in order to maximize the energy yield. Catering for more PV installations requires to advance the power control schemes as well as the regulations in order to avoid adverse impacts from PV systems like overloading the power grid [1]–[3]. For instance, in the *German Federal Law: Renewable Energy Sources Act*, the PV systems with the rated power below 30 kWp have to be able to limit the maximum feed-in power (e.g. 70 % of the rated power) unless it can be remotely controlled by the utility [4]. Such an active power control is referred to as a Constant Power Generation (CPG) control or an absolute power control like described in the Danish grid code [5].

Fundamentals of the CPG concept have been presented in [3], [6], which reveals that the most cost-effective way to achieve the CPG control is by modifying the MPPT algorithm at the PV inverter level. Specifically, the PV system is operated in the MPPT mode, when the PV output power P_{pv} is below the setting-point P_{limit}. However, when the output power reaches P_{limit}, the output power of the PV system will be kept constant, i.e., $P_{\text{pv}} = P_{\text{limit}}$, and leading to a constant active power injection as shown in (1) and illustrated in Fig. 1.

$$P_{\text{pv}} = \begin{cases} P_{\text{MPPT}}, & \text{when} \quad P_{\text{pv}} \le P_{\text{limit}} \\ P_{\text{limit}}, & \text{when} \quad P_{\text{pv}} > P_{\text{limit}} \end{cases} \tag{1}$$

In terms of the algorithms, the CPG based on a Perturb and Observe (P&O-CPG) algorithm was introduced in single-stage PV systems [7]. However, the operating area of the CPG control is limited to be at the right side of the Maximum Power Point (MPP) of the PV arrays (CPP-R), due to the single-stage configuration. Unfortunately, this decreases the robustness of the control algorithm when the PV systems experience a fast decrease in the irradiance. The operating point may go to the open-circuit condition as illustrated in Fig. 2. This drawback applies also to other CPG algorithms presented in [8] and [9], since all the control algorithms regulate the PV power P_{pv} at the right side of the MPP.

To tackle the above issues, a two-stage grid-connected PV is employed to extend the operating area of the P&O-CPG algorithm. By regulating the PV output power at the left side of the MPP (CPP-L) in Fig. 2, a stable CPG operation is always achieved, since the operating point will never "fall off the hill" during a fast decrease in the irradiance. Thus, the P&O-CPG algorithm can be applied to any two-stage single-phase PV system [10]. This paper is organized as follows: the operational principle of the P&O-CPG algorithm is discussed in Section II, where the dynamics of the P&O-CPG algorithm are analyzed. In Section III, a high-performance CPG algorithm is proposed. Both the conventional and the proposed P&O-CPG algorithms are verified and compared experimentally.

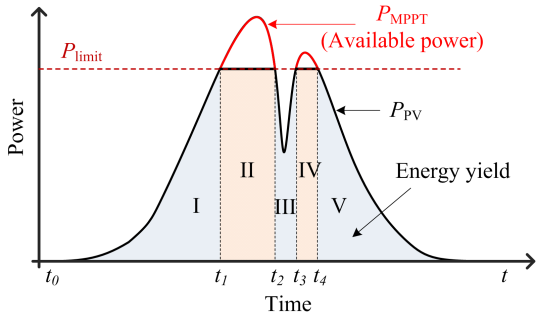

Fig. 1. Constant Power Generation (CPG) concept: 1) MPPT mode during I, III, V, and 2) CPG mode during II, IV [6].

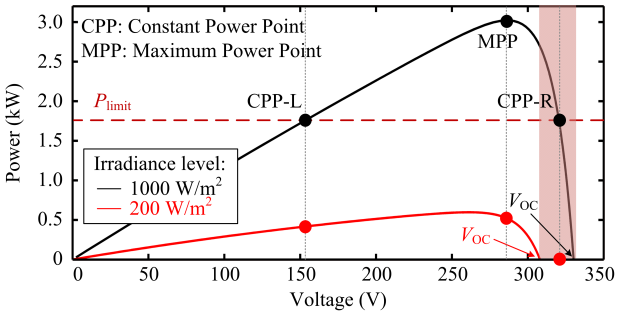

Fig. 2. Stability issues of the conventional CPG algorithms, when the operating point is normally located at the right side of the MPP.

Manuscript received July 3, 2015; revised July 19, 2015; accepted August 1, 2015. Recommended for publication by Associate Editor: XXX. This is the preprint version of a paper accepted in IEEE Transactions on Power Electronics.

The authors are with the Department of Energy Technology, Aalborg University, DK-9220 Aalborg, Denmark (e-mail: ars@et.aau.dk; yoy@et.aau.dk; fbl@et.aau.dk).

Color versions of one or more of the figures in this paper are available online at http://ieeexplore.ieee.org

Digital Object Identifier 10.1109/TPEL.2015.xxxxx

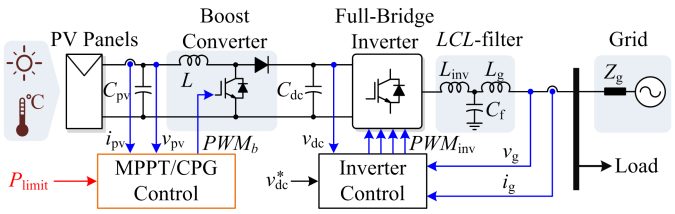

Fig. 3. Hardware schematic and overall control structure of a two-stage single-phase grid-connected PV system.

II. Conventional CPG Algorithm

A. System Configuration

Fig. 3 shows the basic hardware configuration of a two-stage single-phase grid-connected PV system and its control structure. The CPG control is implemented in the boost converter, which will be described in the next section. The control of the full-bridge inverter is realized by using a cascaded control where the DC-link voltage is kept constant through the control of the AC grid current, which is an inner loop [11]. Notably, only an active power is injected to the grid, meaning that the PV system operates at a unity power factor.

Notably, as it has been mentioned above, the two-stage configuration can extend the operating range of both the MPPT and CPG algorithms. In the two-stage case, the PV output voltage $v_{\rm pv}$ can be lower (e.g., at the left side of the MPP), and then it can be stepped up by the boost converter to match the required DC-link voltage (e.g., 450 V) [10]. This is not the case for the single-stage configuration, where the PV output voltage $v_{\rm pv}$ is directly fed to the PV inverter and has to be higher than the grid voltage level (e.g., 325 V) to ensure the power delivery [12].

B. Operational Principle

The operational principle of the conventional P&O-CPG algorithm is illustrated in Fig. 4. It can be divided into two modes: a) MPPT mode ($P_{\rm pv} \le P_{\rm limit}$), where the P&O algorithm should track the maximum power; b) CPG mode ($P_{\rm pv} > P_{\rm limit}$), where the PV output power is limited at $P_{\rm limit}$. During the MPPT operation, the behavior of the algorithm is similar to the conventional P&O MPPT algorithm - the operating point will track and oscillate around the MPP [13]. In the case of the CPG operation, the PV voltage $v_{\rm pv}$ is continuously perturbed toward a point referred to as Constant Power Point (CPP), i.e., $P_{\rm pv} = P_{\rm limit}$. After a number of iterations, the operating point will reach and oscillate around the CPP. Although the PV system with the P&O-CPG control can operate at both CPPs, only the operation at the left side of the MPP (CPP-L) is focused for the stability concern. The control structure of the algorithm is shown in Fig. 5, where $v^*_{\rm pv}$ can be expressed as

$$v^*_{\rm pv} = \begin{cases} v_{\rm MPPT}, & \text{when} \quad P_{\rm pv} \le P_{\rm limit} \\ v_{\rm pv,n} - v_{\rm step}, & \text{when} \quad P_{\rm pv} > P_{\rm limit} \end{cases} \tag{2}$$

where $v_{\rm MPPT}$ is the reference voltage from the MPPT algorithm (i.e., the P&O MPPT algorithm), $v_{\rm pv,n}$ is the measured PV voltage, and $v_{\rm step}$ is the perturbation step size.

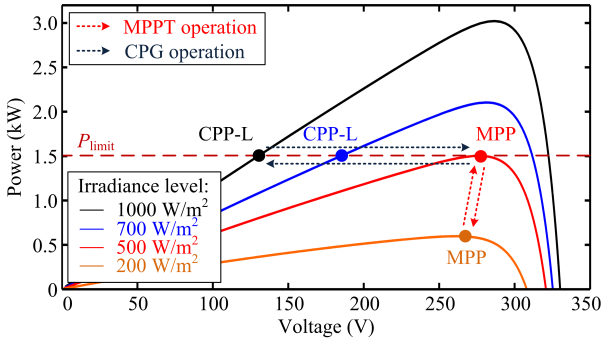

Fig. 4. Operational principle of the Perturb and Observe based CPG algorithm (P&O-CPG), where the operating point is regulated to the left side of the MPP considering stability issues.

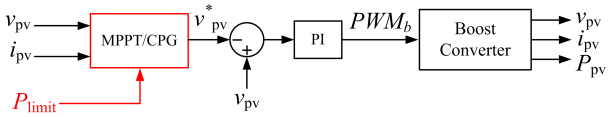

Fig. 5. Control structure of the Perturb and Observe based CPG algorithm (P&O-CPG), where a Proportional Integrator (PI) is adopted.

C. Issues of the P&O-CPG Algorithm

The P&O-CPG algorithm has a satisfied performance under slow changing irradiance conditions, e.g., during a clear day, when the operating point is at the left side of the MPP, as shown in Fig. 6(a). However, irradiance fluctuation that may happen in a cloudy day will result in overshoots and power losses as shown in Fig. 6(b). This can be further explained using the operation trajectory of the PV system presented in Fig. 7. Assuming that the PV system is operating in MPPT mode initially and the irradiance level suddenly increases, the PV power $P_{\rm pv}$ is basically lifted by the change in the irradiance, as it can be seen from the black arrow trajectory (i.e., A→B→C). As a consequence, large power overshoots may occur. Similarly, if the PV system is operating in the CPG operation (e.g., at CPP-L) and the irradiance suddenly drops, the output power $P_{\rm pv}$ will make a sudden decrease, as shown in Fig. 7 (i.e., C→D). It will take a number of iterations until the operating point reaches the new MPP (i.e., E) at that irradiance condition (i.e., 200 W/m^2), and resulting in loss of power generation.

III. High-Performance P&O-CPG Algorithm

According to the above, two main tasks exist - minimizing the overshoots and minimizing the power losses during the fast changing irradiance condition which has to be addressed in the case of CPG operation. The proposed high-performance P&O-CPG algorithm can effectively solve those issues.

A. Minimizing Overshoots

Increasing the perturbation step size is a possibility to minimize the overshoots as the tracking speed is increased. Specifically, a large step size can reduce the required number of iterations to reach the corresponding CPP. Notably, the step size modification should be enabled only when the algorithm

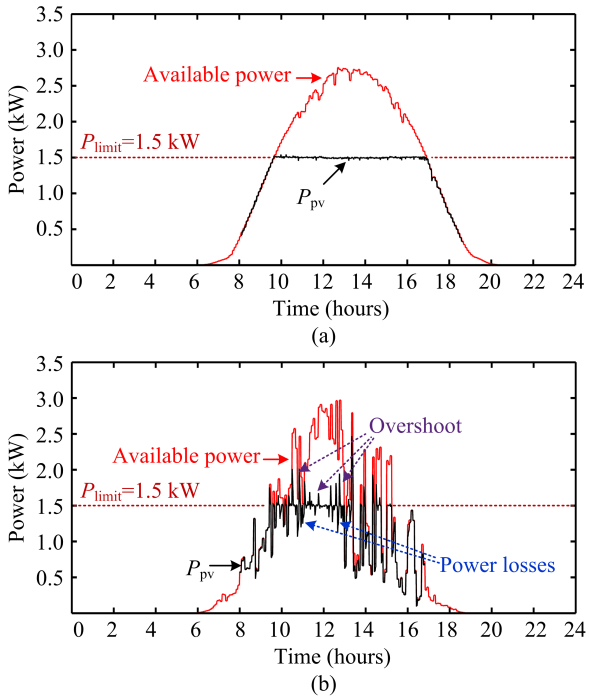

Fig. 6. Experimental results of the Perturb and Observe based CPG algorithm (P&O-CPG) under two daily conditions: (a) clear day and (b) cloudy day.

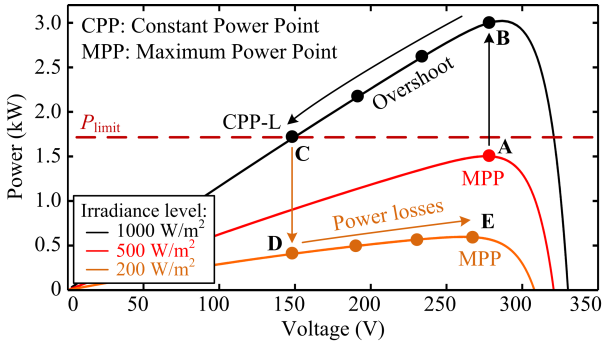

Fig. 7. Operating trajectory of the algorithm during a fast changing irradiance condition resulting in overshoot (black arrow) and power losses (orange arrow).

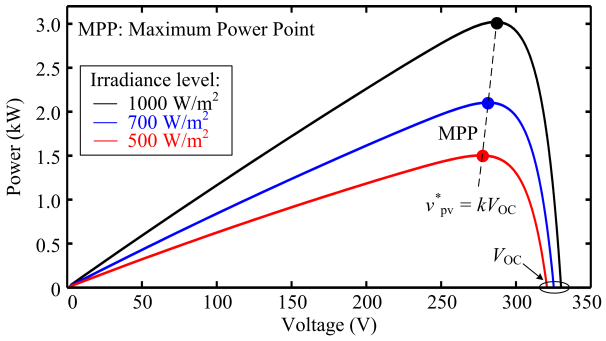

Fig. 8. Power-voltage (P-V) curves of the PV arrays, where the voltage at the MPP is almost constant especially at a higher irradiance level [13].

detects a fast increase in the Irradiance Condition (IC), which can be illustrated as

$$\text{IC} = \begin{cases} 1, & \text{when} \quad P_{\text{pv,n}} - P_{\text{limit}} > \varepsilon_{\text{inc}} \\ 0, & \text{when} \quad P_{\text{pv,n}} - P_{\text{limit}} \leq \varepsilon_{\text{inc}} \end{cases} \tag{3}$$

with $P_{\text{pv,n}}$ being the measured PV power at the present sampling, and ε_{inc} being the criterion, which should be larger than the steady-state power oscillation of the PV panels. When a fast increase in the IC is detected (i.e., IC = 1), an adaptive step size is then employed, where the step size is calculated based on the difference between P_{limit} and $P_{\text{pv,n}}$ as it is given in (4). By doing so, the large step size will be used initially and the step size will continuously be reduced as the operating point approaches to the CPP.

$$v^*_{\text{pv}} = v_{\text{pv,n}} - \left[(P_{\text{pv,n}} - P_{\text{limit}}) \frac{P_{\text{limit}}}{P_{\text{mp}} \cdot \gamma} \right] \cdot v_{\text{step}} \tag{4}$$

where v^*_{pv} is the reference output voltage of the PV arrays, $v_{\text{pv,n}}$ and $P_{\text{pv,n}}$ are the measured output voltage and power of the PV array at the present sampling, respectively. P_{mp} is the rated power. v_{step} is the original step size of the P&O-CPG algorithm. The term $P_{\text{limit}}/P_{\text{mp}}$ is introduced to alleviate the step size dependency in the level of P_{limit}. γ is a constant which can be used to tune the speed of the algorithm.

B. Minimizing Power Losses

As explained in Fig. 7, when the CPG operating point is at the left side of the MPP, the P&O-CPG algorithm requires a number of iterations to reach the new MPP during a fast decease in irradiance, leading to power losses. In fact, the operating point of the PV system does not change much if the PV system is operating in the MPPT under different irradiance levels as shown in Fig. 8. Notably, the detection of the decreased IC as well as the Previous Operating Mode (POM) is also important for minimizing the power losses:

$$\text{IC} = \begin{cases} 1, & \text{when} \quad P_{\text{pv,n-1}} - P_{\text{pv,n}} > \varepsilon_{\text{dec}} \\ 0, & \text{when} \quad P_{\text{pv,n-1}} - P_{\text{pv,n}} \leq \varepsilon_{\text{dec}} \end{cases} \tag{5}$$

$$\text{POM} = \begin{cases} \text{CPG}, & \text{when} \quad |P_{\text{limit}} - P_{\text{pv,n-1}}| < \varepsilon_{\text{ss}} \\ \text{MPPT}, & \text{when} \quad |P_{\text{limit}} - P_{\text{pv,n-1}}| \geq \varepsilon_{\text{ss}} \end{cases} \tag{6}$$

where ε_{dec} and ε_{ss} are criteria to determine the fast irradiance decrease and the CPG operating mode, respectively. $P_{\text{pv,n-1}}$ is the measured PV power at the previous sampling. For example, the value of ε_{ss} can be chosen as 1-2 % of the rated power of the PV system, which is normally higher than the steady-state error in the PV power of the P&O-CPG algorithm.

When a fast decrease (i.e., IC = 1) is detected during the CPG to MPPT transition according to (6), a constant voltage given by (7) is applied to the PV system in order to accelerate the tracking speed (i.e., minimize the power losses). The constant voltage can be approximated as 71-78 % of the open-circuit voltage V_{OC}, as illustrated in Fig. 8 [13].

$$v^*_{\text{pv}} = k \cdot V_{\text{OC}}, \quad \text{where} \quad 0.71 \leq k < 0.78. \tag{7}$$

By doing so, the operating point can be instantaneously moved close to the MPP (in Fig. 7, i.e., D→E) in one perturbation, resulting in a significant reduction in the number of iterations until the operating point reaches the MPP. This approach is simple but effective, which is very suitable to be implemented.

TABLE I
PARAMETERS OF THE TWO-STAGE SINGLE-PHASE PV SYSTEM (FIG. 3).

Boost converter inductor	L = 1.8 mH
PV-side capacitor	C_{pv} = 1000 μF
DC-link capacitor	C_{dc} = 1100 μF
LCL-filter	L_{inv} = 4.8 mH, L_{g} = 4 mH, C_f = 4.3 μF
Switching frequency	Boost converter: f_b = 16 kHz, Full-Bridge inverter: f_{inv} = 8 kHz
DC-link voltage	V_{dc} = 450 V
Grid nominal voltage (RMS)	V_g = 230 V
Grid nominal frequency	ω_0 = 2$\pi\times$50 rad/s

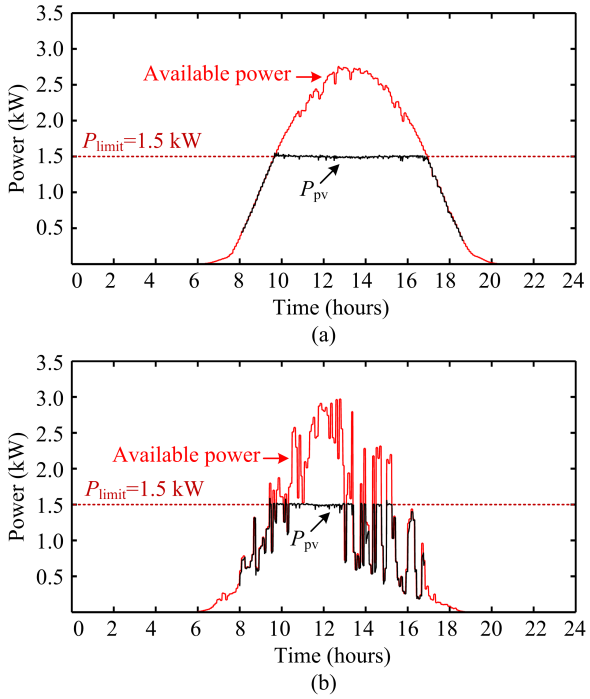

Fig. 9. Experimental results of the proposed high-performance P&O-CPG algorithm under two daily conditions: (a) clear day and (b) cloudy day.

C. Experimental Verification

Solutions to improve the dynamic performance of the P&O-CPG algorithm have been discussed above. Parameters of the proposed high-performance P&O-CPG algorithm are designed as: γ = 10, k = 0.715, ε_{inc} = 50 W, ε_{dec} = 100 W, and ε_{ss} = 30 W. Experiments are carried out referring to Fig. 3, and the system parameters are given in Table I. In the experiments, a 3-kW PV simulator has been adopted, where real-field solar irradiance and ambient temperature profiles are programmed.

Fig. 9 shows the performance of the proposed high-performance P&O-CPG method with two real-field daily conditions. In contrast to the conventional P&O-CPG method (shown in Fig. 6), the overshoots and power losses are significantly reduced by the proposed solution and a stable operation is also maintained. The algorithm also has a selective behavior to only react, when the fast irradiance condition is detected. This can be seen from the performance under clear irradiance conditions in Fig. 9(a), which is similar to the conventional P&O-CPG algorithm (shown in Fig. 6(a)).

IV. CONCLUSION

A high-performance active power control scheme by limiting the maximum feed-in power of PV systems has been proposed in this letter. The proposed solution can ensure a stable constant power generation operation. Compared to the traditional methods, the proposed control strategy forces the PV systems to operate at the left side of the maximum power point, and thus it can achieve a stable operation as well as smooth transitions. Experiments have verified the effectiveness of the proposed control solution in terms of reduced overshoots, minimized power losses, and fast dynamics. Notably, for single-stage PV systems, the same CPG concept is also applicable. However, in that case, the PV voltage operating range is limited and minor changes in the algorithms are necessary to ensure a stable operation.

REFERENCES

[1] T. Stetz, F. Marten, and M. Braun, "Improved low voltage grid-integration of photovoltaic systems in Germany," *IEEE Trans. Sustain. Energy*, vol. 4, no. 2, pp. 534–542, Apr. 2013.
[2] A. Ahmed, L. Ran, S. Moon, and J.-H. Park, "A fast PV power tracking control algorithm with reduced power mode," *IEEE Trans. Energy Conversion*, vol. 28, no. 3, pp. 565–575, Sept. 2013.
[3] Y. Yang, H. Wang, F. Blaabjerg, and T. Kerekes, "A hybrid power control concept for PV inverters with reduced thermal loading," *IEEE Trans. Power Electron.*, vol. 29, no. 12, pp. 6271–6275, Dec. 2014.
[4] *German Federal Law: Renewable Energy Sources Act (Gesetz fur den Vorrang Erneuerbarer Energien) BGBl*, Std., July 2014.
[5] Energinet.dk, "Technical regulation 3.2.5 for wind power plants with a power output greater than 11 kw," Tech. Rep., 2010.
[6] Y. Yang, F. Blaabjerg, and H. Wang, "Constant power generation of photovoltaic systems considering the distributed grid capacity," in *Proc. of APEC*, pp. 379–385, Mar. 2014.
[7] R. G. Wandhare and V. Agarwal, "Precise active and reactive power control of the PV-DGS integrated with weak grid to increase PV penetration," in *Proc. of PVSC*, pp. 3150–3155, Jun. 2014.
[8] W. Cao, Y. Ma, J. Wang, L. Yang, J. Wang, F. Wang, and L. M. Tolbert, "Two-stage PV inverter system emulator in converter based power grid emulation system," in *Proc. of ECCE*, pp. 4518–4525, Sept. 2013.
[9] A. Urtasun, P. Sanchis, and L. Marroyo, "Limiting the power generated by a photovoltaic system," in *Proc. of SSD*, pp. 1–6, Mar. 2013.
[10] S. B. Kjaer, J. K. Pedersen, and F. Blaabjerg, "A review of single-phase grid-connected inverters for photovoltaic modules," *IEEE Trans. Ind. Appl.*, vol. 41, no. 5, pp. 1292–1306, Sept. 2005.
[11] F. Blaabjerg, R. Teodorescu, M. Liserre, and A. V. Timbus, "Overview of control and grid synchronization for distributed power generation systems," *IEEE Trans. Ind. Electron.*, vol. 53, no. 5, pp. 1398–1409, Oct. 2006.
[12] B. Yang, W. Li, Y. Zhao, and X. He, "Design and analysis of a grid-connected photovoltaic power system," *IEEE Trans. Power Electron.*, vol. 25, no. 4, pp. 992–1000, Apr. 2010.
[13] T. Esram and P. L. Chapman, "Comparison of photovoltaic array maximum power point tracking techniques," *IEEE Trans. Energy Conversion*, vol. 22, no. 2, pp. 439–449, Jun. 2007.